Detection of bacterial spoilage during wine alcoholic fermentation using ATR-MIR and MCR-ALS

Julieta Cavaglia, Sílvia Mas Garcia, Jean-Michel Roger, Montserrat Mestres, Ricard Boqué

▶ **To cite this version:**

Julieta Cavaglia, Sílvia Mas Garcia, Jean-Michel Roger, Montserrat Mestres, Ricard Boqué. Detection of bacterial spoilage during wine alcoholic fermentation using ATR-MIR and MCR-ALS. Food Control, 2022, 142, pp.109269. 10.1016/j.foodcont.2022.109269 . hal-03759122

HAL Id: hal-03759122
https://hal.inrae.fr/hal-03759122

Submitted on 25 Aug 2022

HAL is a multi-disciplinary open access archive for the deposit and dissemination of scientific research documents, whether they are published or not. The documents may come from teaching and research institutions in France or abroad, or from public or private research centers.

L'archive ouverte pluridisciplinaire **HAL**, est destinée au dépôt et à la diffusion de documents scientifiques de niveau recherche, publiés ou non, émanant des établissements d'enseignement et de recherche français ou étrangers, des laboratoires publics ou privés.

Distributed under a Creative Commons Attribution - NonCommercial - NoDerivatives 4.0 International License

Food Control 142 (2022) 109269

Contents lists available at ScienceDirect

Food Control

journal homepage: www.elsevier.com/locate/foodcont

Detection of bacterial spoilage during wine alcoholic fermentation using ATR-MIR and MCR-ALS

Julieta Cavaglia [a], Silvia Mas Garcia [b,c], Jean-Michel Roger [b,c], Montserrat Mestres [a], Ricard Boqué [d,*]

[a] Universitat Rovira i Virgili. Instrumental Sensometry (iSens), Department of Analytical Chemistry and Organic Chemistry, Tarragona, 43007, Spain
[b] ITAP, Univ. Montpellier, INRAE, Institut Agro, 34196, Montpellier, France
[c] ChemHouse Research Group, 34196, Montpellier, France
[d] Universitat Rovira i Virgili. Chemometrics, Qualimetrics and Nanosensors Group, Department of Analytical Chemistry and Organic Chemistry, Tarragona, 43007, Spain

ARTICLE INFO

Keywords:
Must grape fermentation
Wine
Bacterial spoilage
Process control
Process analytical technologies (PAT)
Multivariate curve resolution alternating least squares (MCR-ALS)

ABSTRACT

A new methodology is proposed to describe the evolution of the main chemical compounds of grape must during wine alcoholic fermentation using Attenuated Total Reflectance Mid Infrared (ATR-MIR) spectra in combination with Multivariate Curve Resolution Alternating Least-Squares (MCR-ALS). In addition, we have developed a process control strategy to detect differences between fermentations running under Normal Operation Conditions (NOC) and fermentations intentionally spoiled with lactic acid bacteria at the beginning of alcoholic fermentation (MLF) to promote deviations from NOC.

MCR-ALS models on these data showed a good data fit (R^2 = 99.95% and lack of fit = 2.31%). It was possible to resolve the spectral profiles of relevant molecules involved in the alcoholic fermentation process, including the one related to bacterial spoilage (lactic acid). MSPC charts were built based on the concentration profiles obtained from the MCR-ALS models and using T^2 and Q statistics. Spoiled wines showed off-limit values for T^2 after 96 h, making it possible to detect lactic acid bacteria spoilage in early stages of alcoholic fermentation.

Thus, the use of ATR-MIR spectra and MCR-ALS analysis shows a great potential for a rapid control of the state of the alcoholic fermentation process, making it possible to early detect the appearance of undesired molecules during the process, which allows the winemaker to apply corrective measures and obtain a good final product.

1. Introduction

Wine alcoholic fermentation is a complex biological process that involves the transformation of grape must into wine by the action of yeasts. Although the main reaction is the conversion of reducing sugars into ethanol and CO_2, many other secondary products are obtained throughout the process, some of them of major enological importance such as glycerol, organic acids, higher alcohols, esters and other volatile compounds, conferring the special characteristics to each wine (Ribéreau-Gayon et al., 2006).

The amount of ethanol and other secondary products in the final wine will depend on several factors, including the region were the vineyard is located, the grape variety, the yeast species used, the availability of nutrients and the fermentation conditions. Consequently, the high variability involved makes alcoholic fermentation a difficult process to control (Sablayrolles, 2009). In a winery, the daily measurement of quality control parameters is required to ensure the correct evolution of the process. This usually includes density, pH, temperature and sensory evaluation from an oenological expert. Nevertheless, additional chemical information is needed during the fermentation process in order to avoid unexpected deviations. The analyses required are time consuming and more so when the winery does not have its own analytical laboratory and the wine samples during fermentation must be sent to an external laboratory. This involves obtaining delayed results and therefore reducing the chances of taking correctives measures in time, especially when a deviation is suspected (Bisson & Butzke, 2000).

In wine fermentation, one of the most important deviations are promoted by bacterial spoilage which occurs as different bacteria may be found in the winery environment and can contaminate the grape must during fermentation (Barata et al., 2012). For this reason, most wineries add sulphites into the fermentation tanks as a preventive measure, to

* Corresponding author.
E-mail address: ricard.boque@urv.cat (R. Boqué).

https://doi.org/10.1016/j.foodcont.2022.109269
Received 26 April 2022; Received in revised form 29 June 2022; Accepted 17 July 2022
Available online 21 July 2022
0956-7135/© 2022 The Authors. Published by Elsevier Ltd. This is an open access article under the CC BY-NC-ND license (http://creativecommons.org/licenses/by-nc-nd/4.0/).

avoid the growth of unwanted bacteria that may have a detrimental effect on the quality of the final wine (Ough, 1986). Although the content of sulphites is clearly regulated and cannot exceed 150 mg/L in red wines or 200 mg/L in white wines, the food intolerance that it produces in some people is causing health concerns. Thus, most wineries are trying to add as less sulphites as possible, or even produce "sulphite--free" wines (Ubeda et al., 2020).

One example of deviation promoted by bacterial spoilage is malolactic fermentation, which is produced by lactic acid bacteria (LAB). This process involves the transformation of malic acid (a diprotic acid) into lactic acid (a monoprotic acid), resulting in the deacidification of the wine. Usually, in white wines and in some red wines, this increase in pH is not desirable, as it causes a loss of freshness notes (Fugelsang & Edwards, 2007).

Therefore, the monitoring of alcoholic fermentation by means of fast analytical tools is necessary to detect the possible deviations and, specifically, vibrational spectroscopy has shown its suitability for this purpose (dos Santos et al., 2017). Using mid infrared (MIR) spectroscopy, good prediction values ($R^2 > 0.99$) were obtained for important fermentation compounds including glucose, fructose and alcoholic degree (Cozzolino et al., 2011; Fayolle et al., 1996; Urtubia et al., 2004). Furthermore, the determination of other important parameters, such as total titratable acidity and total phenolic compounds, has also been investigated, with low prediction errors (Fragoso et al., 2011; Picque et al., 1993).

Spectroscopic techniques, unlike traditional methods, are fast, nondestructive and usually require a minimum sample pretreatment (Roberts et al., 2018), making them of particular interest as a process analytical technology tool for bioprocess monitoring (e.g. alcoholic fermentation) (Landgrebe et al., 2010). Process analytical technologies (PAT) are a series of guidelines for the monitoring and quality control of products. They were first introduced in 2004 by the American Food and Drug Administration (FDA) and aim at defining manufacturing processes through timely measurements (i.e., during processing) of critical quality and performance attributes of raw and in-process materials (Food and Drug Administration, 2004). PAT tools have been gaining popularity for process and quality control of many food products, including wine (O'Donnell et al., 2009), as process deviations can be detected and, when possible, corrective actions can be taken before the process is complete (Jenzsch et al., 2018).

On the other hand, Partial Least Squares (PLS) regression is considered the most popular regression method for predicting chemical composition during alcoholic fermentation using spectroscopic data (Wold et al., 2001). However, in order to obtain robust calibration models, the analysis of key chemical parameters by traditional methods is required in a significant number of samples during the fermentation process, which is not always feasible (Wold et al., 2001). In addition, wine matrix can contain hundreds of organic compounds, and this makes the analysis and interpretation of infrared spectra an extremely challenging task, especially due to the close similarity among organic compounds, which results in overlapping spectral bands (Craig et al., 2015). Several studies have suggested the use of Multivariate Curve Resolution Alternating Least-Squares (MCR-ALS) on spectroscopic data as a monitoring tool during food processing. Grassi et al. successfully applied MCR-ALS models to ATR-MIR data to describe the evolution of different fermentable sugars and ethanol during beer fermentation, obtaining a good data fit (explained variance >91%) (Grassi et al., 2014a). Similarly, milk fermentation was monitored by applying MCR-ALS to FT-NIR data, obtaining spectroscopic profiles for all phases of milk coagulation and describing the main changes of milk during fermentation (Grassi et al., 2014b). González-Sáiz et al. successfully described the relative concentration profiles and pure spectra of sugars, ethanol and biomass during alcoholic fermentation of onion juice using NIR data and MCR-ALS, reproducing 99.99% of the data and obtaining a low lack of fit (LOF = 0.09%) (González-Sáiz et al., 2008).

In another study, Grassi et al. investigated the application of MCR-ALS to FT-NIR data from the milk renneting process. In their study, MSPC charts based on T^2 and Q statistics from PCA models built on MCR-ALS concentration profiles were able to distinguish coagulation problems in failure batches from the first minutes of the process (Grassi et al., 2019).

Using MCR-ALS, the extraction of relevant information from the MIR spectra during wine alcoholic fermentation allows determining if the process is developing correctly. Because bacterial spoilage of wine is related to the appearance of certain molecules during fermentation, the aim of the present study was to explore the application of MCR-ALS to ATR-MIR data for monitoring wine alcoholic fermentation and detecting undesirable deviations caused by the addition of spoilage bacteria. This paper has two main objectives. First, to describe, using MCR-ALS models, the evolution of the concentrations of the main chemical compounds (sugars and ethanol) in wine fermentation and the appearance of a new compound (lactic acid) originating from lactic acid bacteria spoilage. Second, to evaluate if the information from the MCR-ALS models could be used as a process control tool to detect possible deviations during wine alcoholic fermentation.

2. Materials and methods

2.1. Microvinifications

As in previous studies (Cavaglia et al., 2020), a batch of small-scale alcoholic fermentations (microvinifications) was performed using a concentrated white grape must (Mostos Españoles S.A, Ciudad Real, Spain). The must was defrosted and diluted to a final sugar (glucose and fructose) concentration of 200 ± 10 g L^{-1}. Microvinifications were performed in 500 mL conical flasks by adding 350 mL of diluted must. A total of 18 microvinifications were performed: 10 running in Normal Operation Conditions (NOC), and 8 with an induced contamination of lactic acid bacteria (LAB). For all fermentations, yeast assimilable nitrogen was adjusted by supplementation with 0.30 g L^{-1} of ENOVIT (SPINDAL, S.A.R.L. Gretz-Armainvilliers, France) and 0.30 g L^{-1} of Actimaxbio* (Agrovin, Ciudad Real, Spain). All flasks were inoculated with the commercial dry yeast strain *Saccharomyces cerevisiae* "E491" (Vitilevure Albaflor, YSEO, Danstar Ferment A.G., Denmark), reaching a final concentration of $3{\cdot}10^6$ CFU mL^{-1}. To simulate the bacterial contaminations, the spoiled microvinifications were obtained by adding a freeze-dried blend of LAB (*Lactobacillus plantarum* and *Oenococcus oeni*, Anchor Oenology, Montpellier, France) reaching two different concentrations: $2.5{\cdot}10^6$ and $4{\cdot}10^6$ CFU mL^{-1} (for LAB1 and LAB2, respectively). Adding different concentrations of bacteria induces the malolactic fermentation deviations to start at different points of the alcoholic fermentation (the higher the concentration, the earlier the deviation will appear).

2.2. Fermentation monitoring

All the microvinifications were kept at 18 °C and density was measured at different time points until the end of alcoholic fermentation (density >0.995 g L^{-1}) to control the correct evolution of the process. After homogenization, 1.5 mL were collected at least once a day and centrifuged at 10000 rpm (G-force = 448) for 10 min, to avoid the scattering effect produced by the microorganisms present in the sample. The pellet was discarded and the supernatant was kept in 2 mL eppendorfs for further analysis. Malolactic fermentation ended when the L-malic acid concentration was under 0.06 g L^{-1}. Density measurements were made with a portable densimeter (Densito2Go, Mettler Toledo, United States). L-malic acid content was measured using a Y15 Analyser (Biosystems, Barcelona, Spain). All the analyses were performed right after sample collection.

2.3. ATR-MIR analysis

Infrared measurements were performed with a portable 4100 ExoScan FTIR spectrometer (Agilent, California, USA), equipped with an interchangeable spherical ATR sampling interface with a diamond crystal window. The spectroscopic range was from 4000 to 650 cm^{-1}, and spectra were recorded with a resolution of 8 cm^{-1} and 32 scans. An air-background was collected before each sample to avoid interferences due to the variation in room conditions. All samples were measured in triplicate. From each one of the 2 mL eppendorfs, a drop of the sample was placed on top of the crystal and the spectrum was recorded immediately afterwards. Spectra were collected using the Microlab PC software (Agilent, California, USA) and data were saved as.spc files. The mean of the triplicates was used in subsequent data analysis.

2.4. Data preprocessing

Data preprocessing is usually required to allow the extraction of chemical/physical information and attenuate undesirable signal contributions from the samples and/or the instrument. In the present work, a common preprocessing for spectral data was used: combination of Savitzky–Golay (SG) smoothing (Savitzky & Golay, 1964) with standard normal variate (SNV) transformation (Barnes et al., 1989).

The smoothing parameters in SG (15-point-window smoothing, first-order polynomial degree) were selected to keep the spectral features contained in the original spectra. Scattering effects were reduced by applying SNV. Moreover, in order to minimize the influence of sugars in the data and because our objective was to focus on the absorptions from bonds of organic acids (i.e. lactic acid), the spectroscopic region between 1309 and 1082 cm^{-1} was selected for further analysis. This wavenumber range falls in the fingerprinting region of the mid-infrared spectrum and is related to the absorption of several bonds that are characteristic of organic acids (C–O and C–C stretching, $–CH_2$ and $–CH_3$ bonds) (Picque et al., 2010; Vigentini et al., 2014).

2.5. Multivariate curve resolution-alternating least squares (MCR-ALS)

Every *i*th fermentation experiment monitored by ATR-MIR provides a data matrix, $\mathbf{D}_i$ (K x J), where rows (K) are the spectra collected at different k process times and the columns (J) are the spectral wavelengths. The **D** matrix is defined by the following bilinear model:

$$\mathbf{D} = \mathbf{C}\cdot\mathbf{S}^{\mathrm{T}} + \mathbf{E} \quad (1)$$

where **C** (K x F) is the matrix of the kinetic profiles of the resolved compounds (F), $\mathbf{S}^{\mathrm{T}}$ (F x J) is the matrix containing the resolved pure spectral profiles, and **E** (K x J) is the residual matrix containing the data unexplained by the bilinear model.

In order to obtain a more complete information about the different fermentations, all acquired ATR-MIR data (for all fermentation samples, I) were treated together. For this purpose, all $\mathbf{D}_i$ data matrices were arranged into a new augmented data matrix, setting one on top of each other and keeping the common wavelengths in the same column. The bilinear model in Equation (1) is now extended as shown in Equation (2) and Fig. 1.

$$\mathbf{D}_{\mathrm{aug}} = [\mathbf{D}_1;\mathbf{D}_2;\ldots;\mathbf{D}_I] = [\mathbf{C}_1;\mathbf{C}_2;\ldots;\mathbf{C}_I]\cdot\mathbf{S}^{\mathrm{T}} + [\mathbf{E}_1;\mathbf{E}_2;\ldots;\mathbf{E}_I] = \mathbf{C}_{\mathrm{aug}}\cdot\mathbf{S}^{\mathrm{T}} + \mathbf{E}_{\mathrm{aug}} \quad (2)$$

$\mathbf{C_{aug}}$ is a column-wise augmented matrix formed by the $\mathbf{C}_i$ submatrices that contain the resolved spectra at the different process times, and $\mathbf{S}^{\mathrm{T}}$ is a single data matrix of pure spectra, assumed to be common for all the different process times.

Multivariate curve resolution-alternating least squares (MCR-ALS) aims at resolving the underlying bilinear model (see Equations (1) and (2)) by using the sole information contained in the raw data set **D** (or $\mathbf{D}_{\mathrm{aug}}$). The optimization of MCR matrices with ALS involves an iterative approach, which starts from initial estimates of **C** or $\mathbf{S}^{\mathbf{T}}$ that evolve until profiles with chemically meaningful shapes are obtained. The goal of the MCR-ALS iterations is to minimize as much as possible the residuals in the **E** matrix using least-squares and applying suitable constraints. Constraints involve the accommodation of external chemical information (chemical knowledge of the system) into the optimization process, and they are necessary because the product $\mathbf{C}\cdot\mathbf{S}^{\mathrm{T}}$ is subjected to rotational and intensity ambiguities (de Juan et al., 2009; Tauler, 1995).

In this study, MCR-ALS estimated iteratively the matrices $\mathbf{C}_{\mathrm{aug}}$ and $\mathbf{S}^{\mathrm{T}}$ by alternating least squares under the application of the following constraints:

- Non-negativity in the concentration profiles (concentration of the chemical compounds must be positive to have a physicochemical meaning).
- Unimodality in the concentration profiles (presence of a single maximum per profile)
- Normalization of pure spectra (to avoid scale instabilities during ALS optimization and to fix possible intensity ambiguities)

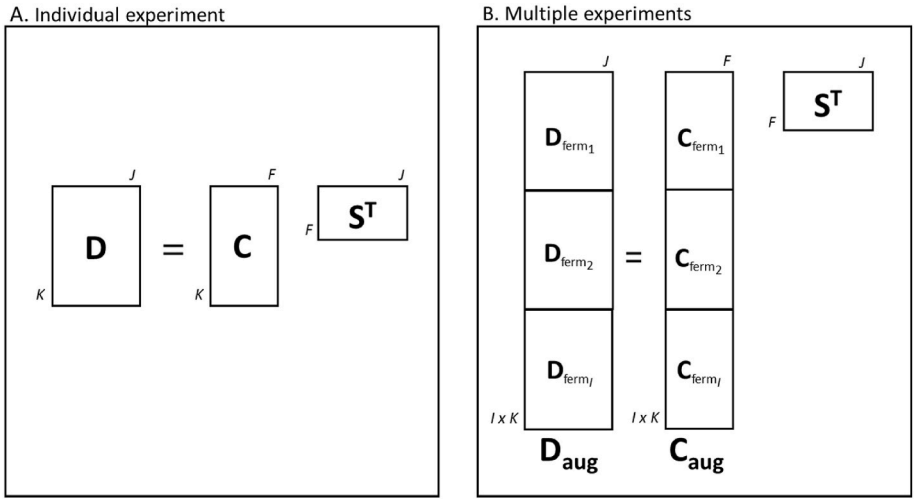

Fig. 1. Bilinear model for the fermentation batches. A. Individual analysis for one single fermentation experiment. B. Simultaneous analysis including different fermentation experiments to build the **C** augmented matrix ($\mathbf{C}_{\mathrm{aug}}$). I refers to the number of experiments, K to the number of time points, J to the number of wavenumbers, and F to the number of components.

- Correspondence among species to encode the information related to the presence/absence of some components in the different $\mathbf{C}_i$ submatrices.

The quality and reliability of the MCR-ALS models were evaluated by calculating two parameters that allow assessing the dissimilarity between the experimental data matrix ($\mathbf{D}_{aug}$) and the data modeled by MCR-ALS. These parameters are the lack of fit (% LOF) and the explained variance (% r2):

$$\%\ \mathrm{LOF} = 100 \times \sqrt{\frac{\Sigma e_{ij}^2}{\Sigma d_{ij}^2}} \tag{3}$$

$$\%\ \mathrm{r2} = 100 \times \left(1 - \frac{\Sigma e_{ij}^2}{\Sigma d_{ij}^2}\right) \tag{4}$$

where d_{ij} is an element of the experimental data matrix $\mathbf{D}_{aug}$ and e_{ij} is the corresponding element of $\mathbf{E}_{aug}$ (Cf **Equation (2)**).

The number of components included in the MCR-ALS model is a compromise between model simplicity, maximum variance explained by the model, and model interpretability. MCR-ALS models were built using the MCR GUI (MCR UB, Barcelona) working under Matlab R2015 (The MathWorks, Natick, USA). More details about the MCR-ALS method are given in (Jaumot et al., 2015) and a GUI to use the algorithm is freely available at http://mcrals.info.

2.6. 'Inverse' MSPC charts

In process control involving multivariate data, MSPC charts are a valuable tool to monitor the effect of different variables at the same time. Due to the high of correlation in spectroscopic data, MSPC methods are usually based on principal component analysis (PCA), where changes in the covariance structure of the process variables are detected. Conventional MSPC-PCA models identify process disturbances as soon as they occur using T^2 and Q statistical limits (Sahni et al., 2005). Typically, a calibration model is developed using data collected from samples running in normal operating conditions (NOC) to define the design-space limits covering the NOC space, and deviations are detected when changes in the covariance matrix occur or abnormal signals arise. The T^2 statistic calculates the distance from an observation to the center of the "in-control" set and determines whether a future observation has a systematic deviation in relation to the samples considered in statistical control. In turn, the Q statistic is defined as the squared Euclidean distance perpendicular to an observation from the subspace defined by PCA and describes how well the PCA model predicts the collected process variable (Chen et al., 2004).

In this study, the idea of 'inverse' MSPC charts is introduced. As explained in the introduction, a fermentation deviation due to lactic acid bacteria spoilage is mainly due to the production of lactic acid. Thus, the modelling of lactic acid production cannot be performed using only NOC batches, as this molecule is not being produced during a normal alcoholic fermentation. First, an MCR-ALS model is built including both NOC and LAB samples ($\mathbf{D}_{augNOCLAB} = [\mathbf{D}_{augNOC};\mathbf{D}_{augLAB}]$):

$$\mathbf{D}_{augNOCLAB} = \mathbf{C}_{augNOCLAB}\cdot\mathbf{S}^T \tag{5}$$

where $\mathbf{C}_{augNOCLAB} = [\mathbf{C}_{augNOC};\mathbf{C}_{augLAB}]$. Then, a PCA model is built only with the **C** matrices of LAB fermentation batches ($\mathbf{C}_{augLAB}$):

$$\mathbf{C}_{augLAB} = \mathbf{T}\cdot\mathbf{P}^T \tag{6}$$

In this way, we ensure that information on lactic acid is being considered in the PCA model. Original $\mathbf{D}_{augNOC}$ spectra are then projected onto the $\mathbf{S}^T$ matrix to obtain new **C** matrices ($\mathbf{C}_{new}$) for NOC batches:

$$\mathbf{C}_{new} = \mathbf{D}_{augNOC}\cdot(\mathbf{S}^T)^+ \tag{7}$$

$\mathbf{C}_{new}$ spectra are projected onto the $\mathbf{C}_{augLAB}$ PCA model, to calculate the score values for the NOC samples:

$$\mathbf{T}_{NOC} = \mathbf{C}_{new}\cdot\mathbf{P} \tag{8}$$

Finally, T^2 values from the scores of the projected $\mathbf{C}_{new}$ spectra ($\mathbf{T}_{NOC}$) are calculated and used in the inverse-MSPC chart. Fig. 2 shows a scheme of the procedure.

3. Results and discussion

3.1. Fermentation monitoring

Fig. 3 shows the average evolution of the measured chemical parameters. Similar behaviors were found for each of the batches in their respective fermentation type (NOC or LAB). Density is an indirect measurement of the content of sugars in the must so the density curves show the typical sigmoidal form of sugar consumption. After 180 h of fermentation, the consumption of sugars was complete for all microvinifications. In the present study, we used malic acid as an indirect measure of lactic acid production. The theoretical balance of malolactic fermentation states that 1 g of malic acid consumed is transformed into 0.672 g of lactic acid and 0.328 g of CO_2. Thus, the theoretical final concentration of lactic acid in the LAB fermentations, from the degradation of 1.6 g L^{-1} of malic acid, is 1.075 g L^{-1} (Larrea Redondo, 1982).

All intentionally contaminated microvinifications produced lactic acid a few hours after the beginning of the alcoholic fermentation, confirming that those fermentations were deviated during the process. During the first 48 h, changes in the concentration of malic acid were very slight. Between the third and fourth day of alcoholic fermentation, the conversion rate of lactic acid increased. In LAB microvinifications, malolactic fermentation ended after 180 h from the beginning of alcoholic fermentation. All NOC fermentations were maintained under control throughout the whole process so less than 0.1 g L^{-1} of malic acid was consumed.

3.2. Multivariate curve resolution

The first MCR-ALS analysis was oriented to identify the specific contributions of both NOC and LAB fermentations. To this aim, two multisets ($\mathbf{D}_{augNOC}$ and $\mathbf{D}_{augLAB}$) were built containing batches related to each particular type of fermentation. MCR-ALS was applied separately to each multiset structure using as constraints non-negativity and unimodality in the concentration profiles and normalization of the spectral profiles.

Table 1 lists the number of resolved components and the explained variance obtained from the MCR-ALS analyses of both multisets. Resolution of three contributions was achieved in both cases. No significant differences between resolved kinetic and spectral profiles of both fermentations (Figure not shown) were found. Therefore, it seems that there is a rank-deficiency phenomenon in LAB fermentations. Rank-deficiency implies that the number of components that can be modeled by MCR-ALS is lower than the actual number of chemical species involved in the reaction (Blanco et al., 2006).

In this case, the rank deficiency in LAB fermentations could be due to the fact that malic and lactic acids have very similar spectra. To overcome this problem, the analysis of a multiset containing all the batches (both NOC and LAB fermentations) was performed. The different information present in the multiset structure enabled a significant improvement of the models, reducing the ambiguities inherent to factor analysis decomposition in the ALS calculation and removing the rank deficiency (Tauler et al., 1995).

Consequently, MCR-ALS was applied to the multiset structure ($\mathbf{D}_{augNOCLAB}$) and four species were resolved. The reliability of the model was very good, with a lack of fit (LOF %) of 2,31% and 99,95% of explained variance,. The addition of a higher number of species

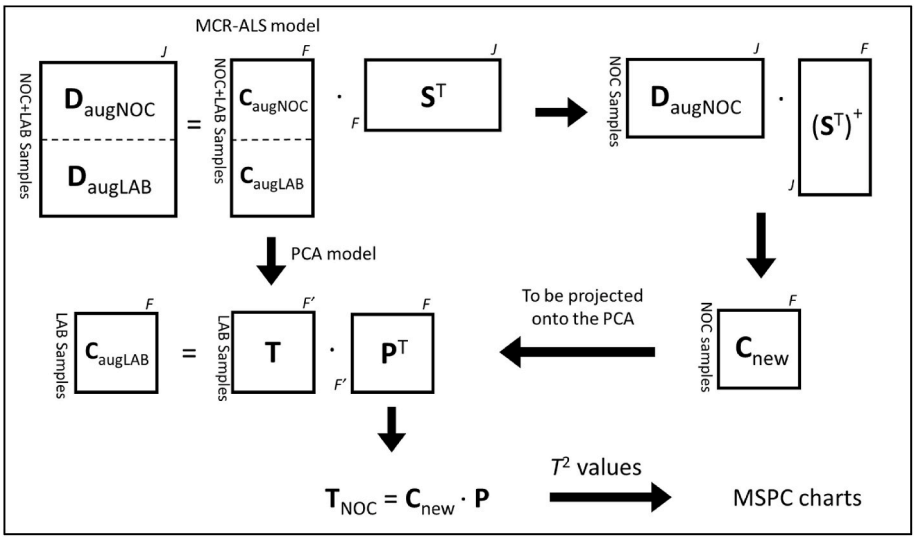

Fig. 2. Scheme of the procedure followed to obtain the 'inverse' MSPC charts. The pseudoinverse of $\mathbf{S}^T$ ($(\mathbf{S}^T)^+$) is used to obtain a $\mathbf{C}_{new}$ matrix from spectroscopic data of control batches ($\mathbf{D}_{augNOC}$).

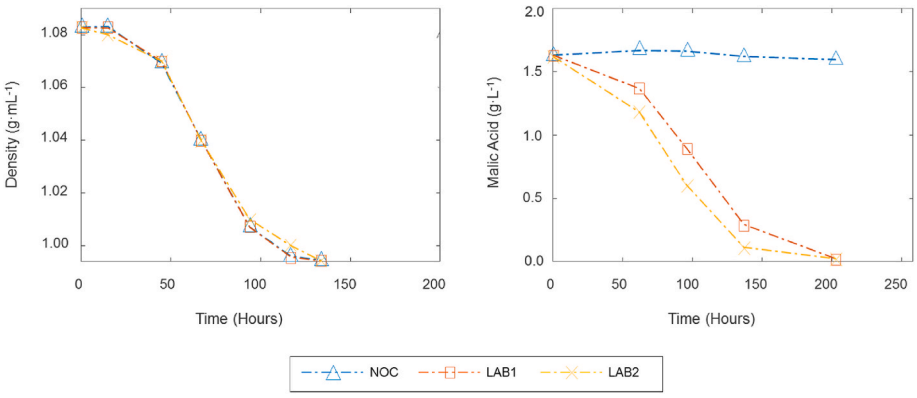

Fig. 3. Evolution of the chemical parameters (density and Malic Acid) measured by reference analysis for the Normal Operation Conditions fermentations (NOC) and the contaminated fermentations (LAB1 and LAB2).

Table 1
Number of resolved components, %LOF and variance explained by MCR-ALS analysis of $\mathbf{D}_{augNOC}$ and $\mathbf{D}_{augLAB}$ multiset structures.

Multiset	Resolved components	Lack of fit (%)	Explained variance (%)
$\mathbf{D}_{augNOC}$	3	1,97	99,96
$\mathbf{D}_{augLAB}$	3	1,27	99,98

provided worse mathematical solutions or unreliable spectra for the concentration profiles. In this case, the constraint of correspondence of species was applied to encode the absence of lactic acid in NOC fermentations.

Fig. 4 shows the $\mathbf{C}_{augNOCLAB}$ matrix for all fermentation batches. All batches showed similar concentration trends for all components, as expected. The profile that decreases (green curve) is related to sugars, which are consumed during alcoholic fermentation. Alcohol is produced from the consumption of sugars and is represented by the curve that increases (red line) a few hours after the beginning of the fermentation. Lactic acid was also simple to assign, given that only LAB fermentations showed the presence of this component (purple line). The curve showing a peak in the middle of the fermentation process (blue line) was more difficult to elucidate. It could be attributed to the presence of salts of tartaric acid, which precipitate by the end of alcoholic fermentation, or intermediate organic species that are part of the yeast metabolism.

In terms of proportion, the ratios obtained by the MCR-ALS are accurate, as the concentration of sugars goes from 200 to <0.05 g L^{-1}, while the concentration of lactic acid goes from zero to approximately 1.075 g L^{-1}, as calculated from theoretical conversion from malic acid. Our results show that MCR-ALS is able to find the relations between major components in wine (ethanol and sugars) and minor components such as lactic acid.

Fig. 5 shows the pure signals ($\mathbf{S}^T$ matrix) obtained for the four components in the MCR-ALS model considering all batches (NOC and LAB microvinifications). Spectral profiles are appropriate as they show absorbance levels in the expected regions for organic compounds. Glucose and fructose were considered as a single species (sugars), as they show a high number of overlapping bands in the MIR region because of their similar chemical structure. Between 1089 and 1126 cm^{-1} spectra are extremely overlapped. In this region C–C and C–H stretching vibrations are found, which are very common in organic molecules. A peak for lactic acid is observed at 1150 cm^{-1}, which can be ascribed to C–O stretching from carboxylic acids (Chapman et al., 2019).

3.3. *Inverse' MSPC charts*

In this study, we propose the development of MSPC charts based on the contaminated samples, rather than on NOC samples. When a sample is projected into the model, if it falls under the "control" limits of the

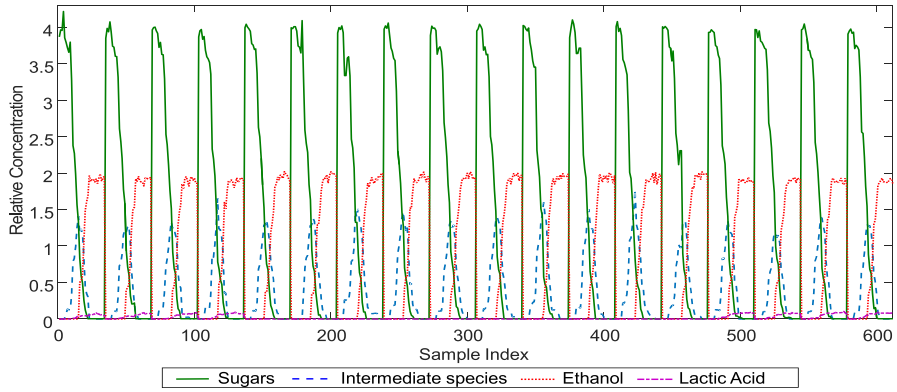

Fig. 4. Relative concentrations for all fermentation batches. The reader is referred to the online version of the paper for legend colors.

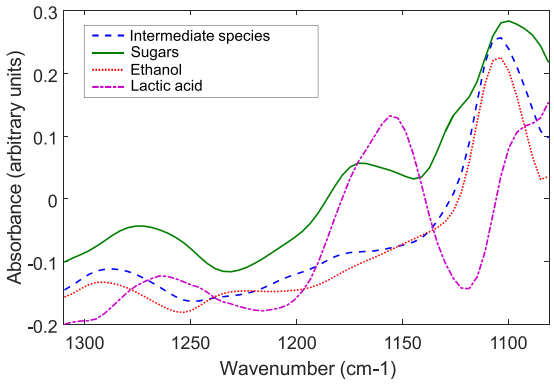

Fig. 5. Pure spectral profiles for the four components in the resulting MCR-ALS model. The reader is referred to the online version of the paper for legend colors.

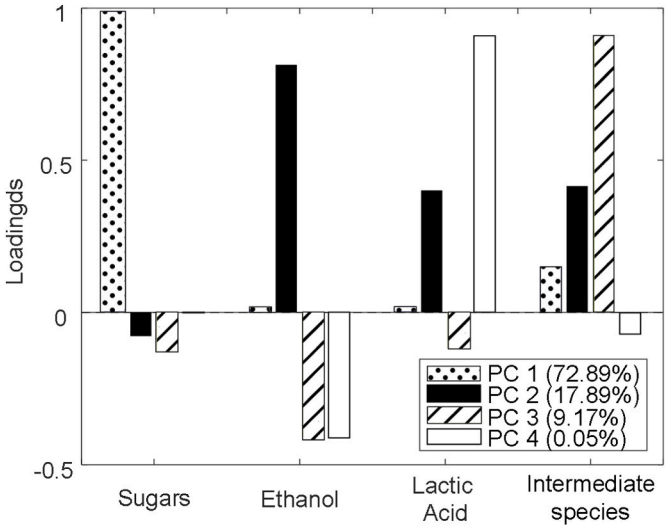

Fig. 6. Loadings for the 4 PCs in the PCA model obtained from the **C** matrix of the MCR-ALS model.

charts, it would mean exactly the opposite from a traditional MSPC chart. Instead of being under control, it would mean that lactic acid is being produced and, therefore, the fermentation should be corrected to return to the normal conditions.

Following the scheme in Fig. 2, a PCA model was built using the $\mathbf{C_{augNOCLAB}}$ matrix, containing all fermentation batches. The $\mathbf{S}^T$ matrix was used to create a new **C** matrix ($\mathbf{C_{new}}$) from the original NOC spectra. Then, the $\mathbf{C_{new}}$ matrix was projected onto the PCA model and the Hotelling T^2 values for these samples were included in the MSPC chart.

Four principal components (PCs) were used to build the PCA model, which explained 100% of the variability in the data, as the projection was made in a four-dimensional space correspoding to the four components resolved by MCR-ALS. Fig. 6 shows the loadings of each PC in this model. In PC1, sugars account for most of the variation, while ethanol is the dominating compound in PC2. In PC3, the intermediate species and ethanol are the most important. Finally, the information on lactic acid is found in PC4.

The 'inverse' MSPC chart based on the Hotelling T^2 statistic is shown in Fig. 7. In this MSPC chart, all samples under the control limits (round shapes) belong to LAB fermentations, were lactic acid is produced during alcoholic fermentation. Between 0 and 60 h, all NOC samples are "under control". This could be explained because during the first 65 h of alcoholic fermentation, the concentration curve for lactic acid does not indicate lactic acid production for both LAC and NOC samples (in this time interval, the production of lactic acid is below the limit of detection of the ATR-MIR instrument). Atypical T^2 values for NOC samples start to appear after 60 h, and all NOC samples are completely out of the limit after 96 h. Hence, ATR-MIR spectra from LAB samples were distinguishable from NOC samples before 100h, which is before the end of

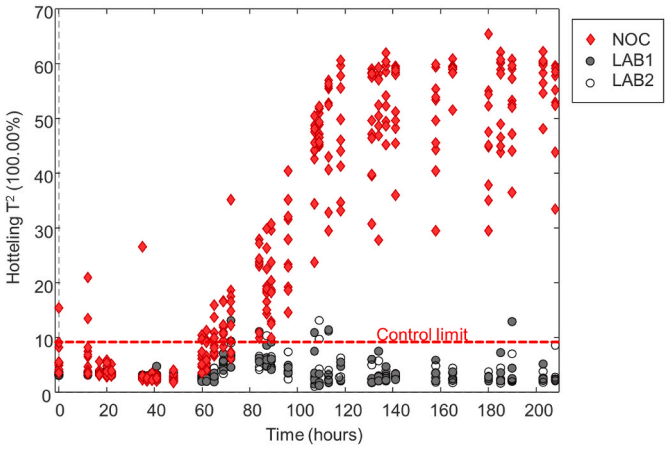

Fig. 7. MSPC chart based on Hotelling T^2, showing the distribution of NOC samples and contaminated LAB1 and LAB2 samples throughout the alcoholic fermentation.

alcoholic fermentation.

Oliveira et al. used local PCA models and were able to build Fixed Size Moving Window MSPC charts and evolving MSPC charts to detect

faulty batches during the distillation process using NIR data (de Oliveira et al., 2017). In our approach, faulty batches are detected using a global PCA model, with no need to build independent PCA models for different times.

4. Conclusions

Our results suggest that ATR-MIR data together with MCR-ALS models and MSPC charts could be used for the detection of lactic acid production during alcoholic fermentation. The use of MCR-ALS with ATR-MIR spectra enables to model the pure kinetic and spectra profiles of the main compounds involved in wine alcoholic and malolactic fermentations. This methodology becomes an improvement of the traditional MSPC charts for bacterial spoilage detection. Thus, if a fermentation batch is out of control in a traditional MSPC chart, but in control in this new 'inverse' MSPC chart, we could conclude not only that the sample is deviated, but also that the fermentation is deviated because of the production of lactic acid, as shown in the relative concentration profiles of MCR-ALS.

CRediT authorship contribution statement

Julieta Cavaglia: Conceptualization, Methodology, Validation, Formal analysis, Investigation, Writing – original draft, Visualization. **Silvia Mas Garcia:** Methodology, Software, Validation, Formal analysis. **Jean-Michel Roger:** Resources, Writing – review & editing, Project administration. **Montserrat Mestres:** Conceptualization, Formal analysis, Investigation, Resources, Writing – review & editing, Supervision, Project administration, Funding acquisition. **Ricard Boqué:** Conceptualization, Methodology, Validation, Investigation, Writing – original draft, Writing – review & editing, Visualization, Supervision, Project administration.

Declaration of competing interest

The authors declare that they have no known competing financial interests or personal relationships that could have appeared to influence the work reported in this paper.

Data availability

Data will be made available on request.

Acknowledgements

Authors would like to thank the scientific advice received from Anna de Juan (Universitat de Barcelona, Spain). Julieta Cavaglia would like to thank to the ChemHouse Research Group (Montpellier, France) for accepting her as a visiting research fellow. Financial support is acknowledged for the *Secretaria d'Universitats i Recerca del Departament d'Empresa i Coneixement de la Generalitat de Catalunya*, the European Union (UE) and the European Social Fund (ESF) (predoctoral fellowship number 2018 FI_B00844), and the Spanish Ministry of Science and Innovation (Project PID2019-104269RR-C33).

References

Barata, A., Malfeito-Ferreira, M., & Loureiro, V. (2012). The microbial ecology of wine grape berries. *International Journal of Food Microbiology, 153*, 243–259. https://doi.org/10.1016/j.ijfoodmicro.2011.11.025

Barnes, R. J., Dhanoa, M. S., & Lister, S. J. (1989). Standard normal variate transformation and de-trending of near-infrared diffuse reflectance spectra. *Applied Spectroscopy, 43*, 772–777. https://doi.org/10.1366/0003702894202201

Bisson, L. F., & Butzke, C. E. (2000). Diagnosis and rectification of stuck and sluggish fermentations. *American Journal of Enology and Viticulture*.

Blanco, M., Castillo, M., Peinado, A., & Beneyto, R. (2006). Application of multivariate curve resolution to chemical process control of an esterification reaction monitored by near-infrared spectroscopy. *Applied Spectroscopy, 60*, 641–647. https://doi.org/10.1366/000370206777670710

Cavaglia, J., Schorn-García, D., Giussani, B., Ferré, J., Busto, O., Aceña, L., Mestres, M., & Boqué, R. (2020). Monitoring wine fermentation deviations using an ATR-MIR spectrometer and MSPC charts. *Chemometrics and Intelligent Laboratory Systems, 201*, Article 104011. https://doi.org/10.1016/j.chemolab.2020.104011

Chapman, J., Gangadoo, S., Truong, V. K., & Cozzolino, D. (2019). Spectroscopic approaches for rapid beer and wine analysis. *Current Opinion in Food Science, 28*, 67–73. https://doi.org/10.1016/j.cofs.2019.09.001

Chen, Q., Kruger, U., Meronk, M., & Leung, A. Y. T. (2004). Synthesis of T2 and Q statistics for process monitoring. *Control Engineering Practice, 12*, 745–755. https://doi.org/10.1016/j.conengprac.2003.08.004

Cozzolino, D., Cynkar, W., Shah, N., & Smith, P. (2011). Feasibility study on the use of attenuated total reflectance mid-infrared for analysis of compositional parameters in wine. *Food Research International, 44*, 181–186. https://doi.org/10.1016/j.foodres.2010.10.043

Craig, A. P., Franca, A. S., & Irudayaraj, J. (2015). Vibrational spectroscopy for food quality and safety screening. In *High throughput screen. Food saf. Assess. Biosens. Technol. Hyperspectral imaging pract. Appl.* (1st ed., pp. 165–194). Elsevier Ltd. https://doi.org/10.1016/B978-0-85709-801-6.00007-1.

Fayolle, P., Picque, D., Perret, B., Latrille, E., & Corrieu, G. (1996). Determination of major compounds of alcoholic fermentation by middle-infrared spectroscopy: Study of temperature effects and calibration methods. *Applied Spectroscopy, 50*, 1325–1330. https://doi.org/10.1366/0003702963904872

Food and Drug Administration. (2004). *Guidance for industry. PAT — a framework for innovative pharmaceutical development, manufacturing, and quality assurance*.

Fragoso, S., Aceña, L., Guasch, J., Mestres, M., & Busto, O. (2011). Quantification of phenolic compounds during red winemaking using FT-MIR spectroscopy and PLS-regression. *Journal of Agricultural and Food Chemistry, 59*, 10795–10802. https://doi.org/10.1021/jf201973e

Fugelsang, K. C., & Edwards, C. G. (2007). Managing microbial growth. In *Wine microbiol.* (pp. 65–81). Boston, MA: Springer. https://doi.org/10.1007/978-0-387-33349-6_5.

González-Sáiz, J. M., Esteban-Díez, I., Rodríguez-Tecedor, S., & Pizarro, C. (2008). Valorization of onion waste and by-products: MCR-ALS applied to reveal the compositional profiles of alcoholic fermentations of onion juice monitored by near-infrared spectroscopy. *Biotechnology and Bioengineering, 101*, 776–787. https://doi.org/10.1002/bit.21939

Grassi, S., Alamprese, C., Bono, V., Casiraghi, E., & Amigo, J. M. (2014b). Modelling milk lactic acid fermentation using multivariate curve resolution-alternating least squares (MCR-ALS). *Food and Bioprocess Technology, 7*, 1819–1829. https://doi.org/10.1007/s11947-013-1189-2

Grassi, S., Amigo, J. M., Lyndgaard, C. B., Foschino, R., & Casiraghi, E. (2014a). Assessment of the sugars and ethanol development in beer fermentation with FT-IR and multivariate curve resolution models. *Food Research International, 62*, 602–608. https://doi.org/10.1016/j.foodres.2014.03.058

Grassi, S., Strani, L., Casiraghi, E., & Alamprese, C. (2019). Control and monitoring of milk renneting using FT-NIR spectroscopy as a process analytical technology tool. *Foods, 8*. https://doi.org/10.3390/foods8090405

Jaumot, J., de Juan, A., & Tauler, R. (2015). MCR-ALS GUI 2.0: New features and applications. *Chemometrics and Intelligent Laboratory Systems, 140*, 1–12. https://doi.org/10.1016/j.chemolab.2014.10.003

Jenzsch, M., Bell, C., Buziol, S., Kepert, F., Wegele, H., & Hakemey, C. (2018). Trends in process analytical technology: Present state in bioprocessing. In B. Kiss, U. Gottschal, & M. Pohlscheidt (Eds.), *New bioprocess. Strateg. Dev. Manuf. Recomb. Antibodies proteins* (1st ed., pp. 211–252). Switzerland: Springer International Publishing.

de Juan, A., Rutan, S. C., & Tauler, R. (2009). Two-way data analysis: Multivariate curve resolution – iterative resolution methods. In R. Brown, B. Tauler, & Walczak (Eds.), *Compr. Chemom.* (pp. 325–344). Amsterdam: Elsevier. https://doi.org/10.1016/B978-044452701-1.00050-8.

Landgrebe, D., Haake, C., Höpfner, T., Beutel, S., Hitzmann, B., Scheper, T., Rhiel, M., & Reardon, K. F. (2010). On-line infrared spectroscopy for bioprocess monitoring. *Applied Microbiology and Biotechnology, 88*, 11–22. https://doi.org/10.1007/s00253-010-2743-8

Larrea Redondo, A. (1982). Enología básica. In *Enol. Básica, AEDOS EDITORIAL.* Barcelona: S.A.

O'Donnell, C., Fagan, C., & Cullen, P. (2009). Process analytical technology for the food industry. In *Process anal. Technol. Food ind.* (2nd ed., pp. 20–30).

de Oliveira, R. R., Pedroza, R. H. P., Sousa, A. O., Lima, K. M. G., & de Juan, A. (2017). Process modeling and control applied to real-time monitoring of distillation processes by near-infrared spectroscopy. *Analytica Chimica Acta, 985*, 41–53. https://doi.org/10.1016/j.aca.2017.07.038

Ough, C. S. (1986). Determination of sulfur dioxide in grapes and wines. *Journal Assoction Office Analysis Chemistry*, 5–7. https://doi.org/10.1093/jaoac/69.1.5

Picque, D., Lefier, D., Grappin, R., & Corrieu, G. (1993). Monitoring of fermentation by infrared spectrometry: Alcoholic and lactic fermentations. *Analytica Chimica Acta, 279*, 67–72. https://doi.org/10.1016/B978-0-444-81640-5.50010-0

Picque, D., Lieben, P., Chrétien, P., Béguin, J., & Guérin, L. (2010). Assessment of maturity of loire valley wine grapes by mid-infrared spectroscopy. *J. Int. Des Sci. La Vigne Du Vin*. https://doi.org/10.20870/oeno-one.2010.44.4.1477

Ribéreau-Gayon, P., Dubourdieu, D., Donèche, B., & Lonvaud, A. (2006). Handbook of enology. In *The microbiology of wine and vinifications* (2nd ed.,, *1*. John Wiley & Sons. https://doi.org/10.1002/0470010363.fmatter

Roberts, J. J., Power, A., Chapman, J., Chandra, S., & Cozzolino, D. (2018). Vibrational spectroscopy methods for agro-food product analysis. *Comprehensive Analytical Chemistry*, 51–68. https://doi.org/10.1016/bs.coac.2018.03.002

Sablayrolles, J. M. (2009). Control of alcoholic fermentation in winemaking: Current situation and prospect. *Food Research International, 42*, 418–424. https://doi.org/10.1016/j.foodres.2008.12.016

Sahni, N. S., Aastveit, A. H., & Naes, T. (2005). In-line process and product control using spectroscopy and multivariate calibration. *Journal of Quality Technology, 37*, 1–20. https://doi.org/10.1080/00224065.2005.11980296

dos Santos, C. A. T., Páscoa, R. N. M. J., & Lopes, J. A. (2017). A review on the application of vibrational spectroscopy in the wine industry: From soil to bottle. *Trends in Analytical Chemistry, 88*, 100–118. https://doi.org/10.1016/j.trac.2016.12.012

Savitzky, A., & Golay, M. J. E. (1964). Smoothing and differentiation of data by simplified least squares procedures. *Analytical Chemistry, 36*, 1627–1639. https://doi.org/10.1021/ac60214a047

Tauler, R. (1995). Multivariate curve resolution applied to second order data. *Chemometrics and Intelligent Laboratory Systems, 30*, 133–146. https://doi.org/10.1016/0169-7439(95)00047-X

Tauler, R., Smilde, A., & Kowalski, B. (1995). Selectivity, local rank, three-way data analysis and ambiguity in multivariate curve resolution. *Journal of Chemometrics, 9*, 31–58. https://doi.org/10.1002/cem.1180090105

Ubeda, C., Hornedo-Ortega, R., Cerezo, A. B., Garcia-Parrilla, M. C., & Troncoso, A. M. (2020). Chemical hazards in grapes and wine, climate change and challenges to face. *Food Chemistry, 314*, Article 126222. https://doi.org/10.1016/j.foodchem.2020.126222

Urtubia, A., Pérez-Correa, J. R., Meurens, M., & Agosin, E. (2004). Monitoring large scale wine fermentations with infrared spectroscopy. *Talanta, 64*, 778–784. https://doi.org/10.1016/j.talanta.2004.04.005

Vigentini, I., Grassi, S., Sinelli, N., Di Egidio, V., Picozzi, C., Foschino, R., & Casiraghi, E. (2014). Near and Mid Infrared Spectroscopy to detect malolactic biotransformation of Oenococcus oeni in a wine-model. *Journal of Agriculture, Science and Technology, 4*, 475–786.

Wold, S., Sjöström, M., & Eriksson, L. (2001). PLS-Regression: A basic tool of chemometrics. *Chemometrics and Intelligent Laboratory Systems, 58*, 109–130. https://doi.org/10.1016/S0169-7439(01)00155-1